Neurobiology of Disease 125 (2019) 146–153

Contents lists available at ScienceDirect

Neurobiology of Disease

journal homepage: www.elsevier.com/locate/ynbdi

Long-term RNAi knockdown of α-synuclein in the adult rat substantia nigra without neurodegeneration

Alevtina Zharikov[a,c], Qing Bai[a,c], Briana R. De Miranda[a,c], Amber Van Laar[a,c], J. Timothy Greenamyre[a,c,d], Edward A. Burton[a,b,c,d,*]

[a] Department of Neurology, University of Pittsburgh, Pittsburgh, PA, USA
[b] Department of Microbiology and Molecular Genetics, University of Pittsburgh, Pittsburgh, PA, USA
[c] Pittsburgh Institute for Neurodegenerative Diseases, University of Pittsburgh, Pittsburgh, PA, USA
[d] Geriatric Research, Education and Clinical Center, Pittsburgh VA Healthcare System, Pittsburgh, PA, USA

A B S T R A C T

α-Synuclein plays a central role in the pathogenesis of Parkinson's disease (PD); interventions that decrease its expression appear neuroprotective in PD models. Successful translation of these observations into effective therapies will be dependent on the safety of suppressing α-synuclein expression in the adult brain. We investigated long-term α-synuclein knockdown in the adult rat CNS. 8-month old animals received either AAV-sh[Snca] (an RNA interference vector targeting the *Snca* mRNA transcript) or AAV-sh[Ctrl] (a control vector) unilaterally into the substantia nigra. No signs of systemic toxicity or motor dysfunction were observed in either experimental group over 12 months. Viral transgene expression persisted to 12 months post-inoculation, at which point *Snca* mRNA expression in substantia nigra dopaminergic neurons of animals that received AAV-sh[Snca] was decreased by ≈90%, and α-synuclein immunoreactivity by > 70% relative to the control side. Stereological quantification of Nissl-labeled neurons showed no evidence of neurodegeneration in the substantia nigra 12 months after inoculation with either vector, and we observed abundant dopaminergic neurons with minimal α-synuclein immunoreactivity that appeared otherwise unremarkable in the AAV-sh[Snca] group. Despite the absence of neurodegeneration, some loss of TH expression was evident in nigral neurons after transduction with either vector, presumably a non-specific consequence of vector delivery, cellular transduction, or expression of shRNA or GFP. We conclude that long-term α-synuclein knockdown in the substantia nigra does not cause significant functional deficits in the ascending dopaminergic projection, or neurodegeneration. These findings are encouraging that it may be feasible to target α-synuclein expression therapeutically in PD.

1. Introduction

α-Synuclein is strongly implicated in the pathogenesis of sporadic Parkinson's disease (PD). Lewy bodies, the pathological hallmark inclusion body of PD, contain aggregated α-synuclein (Spillantini et al., 1997). Rare monogenic PD phenocopies are caused by over-expression of α-synuclein (Chartier-Harlin et al., 2004; Singleton et al., 2003). Genome-wide association studies (Edwards et al., 2010; Satake et al., 2009; Simon-Sanchez et al., 2009) reveal PD-associated single-nucleotide polymorphisms near the SNCA gene encoding α-synuclein. Some of the risk-conferring SNPs are located within enhancer sequences and alter α-synuclein expression levels (Soldner et al., 2016). Other variants in the SNCA gene associated with PD are also known to modulate α-synuclein expression (Cronin et al., 2009; Fuchs et al., 2008). Chronic exposure to drugs thought to increase cellular α-synuclein levels has been reported to be a risk factor for PD, and drugs that reduce α-synuclein expression may decrease PD risk (Mittal et al., 2017). Together, these observations suggest that α-synuclein expression levels in susceptible brain regions are a central determinant of pathogenesis in PD.

In view of this evidence, attention has focused on modulating α-synuclein expression as a therapeutic approach. This concept is supported by several prior studies showing that *Snca*$^{-/-}$ mice lacking α-synuclein were resistant to the mitochondrial inhibitor MPTP (Dauer et al., 2002; Fornai et al., 2005; Klivenyi et al., 2006; Robertson et al., 2004; Schluter et al., 2003), a rare cause of acute Parkinsonism in humans (Langston et al., 1983). The mechanism by which loss of α-synuclein is neuroprotective in this model is unresolved, and may involve decreased uptake of MPP^+ into dopaminergic neurons. More recently, we tested α-synuclein knockdown in a model of sporadic PD that replicates neurodegeneration and endogenous synucleinopathy in response to a PD-relevant proximate trigger. Rats exposed subacutely to the mitochondrial inhibitor rotenone, implicated as an environmental risk factor in PD (Tanner et al., 2011), develop progressive Parkinsonism, selective degeneration of substantia nigra dopaminergic neurons and their striatal terminals, and formation of α-synuclein immunoreactive inclusions that resemble Lewy bodies ultrastructurally (Betarbet et al., 2000; Cannon et al., 2009). We developed a viral short hairpin RNA (shRNA) vector that specifically targets the rat *Snca* mRNA

* Corresponding author at: 7015 Biomedical Sciences Tower 3, 3501 Fifth Avenue, Pittsburgh, PA 15213, USA.
E-mail address: eab25@pitt.edu (E.A. Burton).

https://doi.org/10.1016/j.nbd.2019.01.004
Received 6 September 2018; Received in revised form 16 November 2018; Accepted 14 January 2019
Available online 15 January 2019
0969-9961/ Published by Elsevier Inc.

transcript *in vivo* resulting in 30–40% decrease in α-synuclein expression in the substantia nigra by 3 weeks post-transduction (Zharikov et al., 2015). This modest decrease in α-synuclein expression ameliorated motor dysfunction, loss of substantia nigra dopaminergic neurons and synucleinopathy in the rotenone model of PD (Zharikov et al., 2015). These data suggest that α-synuclein expression levels modulate neuronal susceptibility to environmental exposures implicated in PD, and support the concept that interventions targeting α-synuclein expression may be neuroprotective in PD.

Successful development of therapeutic agents that suppress the expression of α-synuclein in PD-susceptible neuronal groups will be critically dependent on targeting α-synuclein in the adult brain without toxicity. Mouse models provide support for the idea that α-synuclein is non-essential in CNS neurons: *Snca*$^{-/-}$ mice, which express no α-synuclein, show only subtle physiological phenotypes in nigrostriatal dopaminergic function, but no evidence of motor deficits or neurodegeneration (Abeliovich et al., 2000; Cabin et al., 2002). Furthermore, a mouse strain harboring a spontaneous *Snca* gene deletion appears phenotypically normal (Specht and Schoepfer, 2001). However, germline null mutations potentially allow the emergence of developmental compensatory mechanisms that might not occur in the adult brain after downregulating α-synuclein in end-differentiated neurons. Consequently, there has been significant interest in the consequences of targeting α-synuclein expression in the adult CNS. Systemic delivery of small interfering RNA (siRNA) targeting *Snca* mRNA was achieved without toxicity in mice, using exosomes expressing Rabies virus glycoprotein (Cooper et al., 2014). Direct infusion of chemically-modified siRNA into the primate midbrain caused 40–50% knockdown of α-synuclein without cell loss (McCormack et al., 2010). Antisense oligonucleotides conjugated with a triple monoamine reuptake inhibitor (Alarcon-Aris et al., 2018) and siRNA sequences complexed with polyethylenimine (Helmschrodt et al., 2017) have also been reported to decrease α-synuclein expression in the adult mouse brain without causing neurodegeneration. In our prior study, we observed no evidence of motor deficit or neurodegeneration 3 or 6 weeks after delivering short hairpin RNA (shRNA) targeting rat *Snca* using an adeno-associated virus (AAV) vector. In contrast, two studies from another group (Benskey et al., 2018; Gorbatyuk et al., 2010) suggest that AAV-shRNA vectors targeting endogenous rat *Snca* cause degeneration of the substantia nigra. The explanation for these unexpected findings is uncertain, but these studies clearly raise questions that need to be addressed about the safety of α-synuclein knockdown.

In view of the potential translational importance of reducing α-synuclein expression in the adult substantia nigra over a prolonged period of time, we designed experiments to determine whether long-term knockdown of α-synuclein causes neurodegeneration. Using our AAV-shRNA vector at higher doses than our previous study, we showed that > 70% decrease in endogenous α-synuclein was tolerated by substantia nigra dopaminergic neurons for 52 weeks, without clinical evidence of a neurological deficit or pathological evidence of neurodegeneration. By employing an isogenic control vector that does not target *Snca*, we also showed that vector inoculation and long-term shRNA expression cause non-specific toxicities that are not attributable to loss of α-synuclein.

2. Materials and methods

2.1. Viral vectors

Generation and characterization of AAV-sh[Snca] and AAV-sh[Ctrl] were described in detail in our previous work (Zharikov et al., 2015). AAV-sh[Snca] specifically and robustly suppresses expression of *Snca* mRNA in the rat midbrain *in vivo,* without affecting expression of *Sncb* or *Sncg*. Plasmids containing the vector genomes have been deposited at Addgene (plasmid numbers #75437 https://www.addgene.org/75437/ and #75438 https://www.addgene.org/75438/). Vectors were prepared to high titer and purity by plasmid co-transfection in 293 cells, at the University of Pennsylvania vector core. New preparations of both vectors were made for this study; to ensure valid comparison between AAV-sh[Snca] and AAV-sh[Ctrl], all steps from streaking plasmid glycerol stocks to vector manufacture were carried out in parallel for the two vectors.

2.2. Animals

Experiments were approved by the University of Pittsburgh Institutional Animal Care and Use Committee National Institutes of Health and complied with the NIH Guide for the Care and Use of Laboratory Animals. 8 month old male Lewis rats were obtained from Charles River Laboratories, (Wilmington, MA). Animals were anesthetized with isofluorane and 2 μL viral vector suspension infused dorsal to the substantia nigra (−5.8 A/P, ± 2.2 R from bregma, −7.5 V from dura) using a Hamilton syringe with a 30-gauge needle (45° bevel) at a rate of 0.2 μL/min exactly as described previously (Zharikov et al., 2015). Both AAV-sh[Snca] and AAV-[Ctrl] were used at the same concentration, 3.4×10^{12} GC/mL, giving a total vector dose of 6.8×10^{9} GC/site. The postural instability test was carried out as described in our previous work (Cannon et al., 2009). Briefly, the animal was suspended with one forelimb in contact with a horizontal surface covered with sand paper. The animal was advanced forwards until forelimb placement was triggered. The displacement required to provoke forelimb placement was recorded for 3 trials at each time point on each side.

2.3. Histology and microscopy

Animals were deeply anesthetized with pentobarbital (50 mg/kg) and perfused-fixed with PBS and 4% paraformaldehyde. Brains were post-fixed, cryoprotected and sectioned (35 μm) using a sliding freezing-stage microtome. Primary antibodies are shown in Table 1. Bound primary antibody was revealed using either: (i) biotin-conjugated secondary antibody (Fig. 2; biotin-SP-conjugated donkey anti-mouse, cat# 715065151, 1:200 dilution, Jackson ImmunoResearch Laboratoties, Inc., West Crove, PA) with avidin/biotinylated peroxidase (ABC-kit, PK-6100, Vectastain Laboratories, Inc., Burlingame, CA, 94010) and a chromogenic substrate yielding a brown reaction product (DAB, SK-4100, Vectastain Laboratories, Inc., Burlingame, CA); or (ii) fluorophore-conjugated secondary antibodies (Figs. 3, 4; AlexaFluor 488, 555, and 647; 1:500 dilution; ThermoFisher Scientific, Waltham, MA). Low magnification images in Fig. 2 were acquired using an Olympus MVX-10 macro zoom microscope with Spot camera and software (B + B Microscopes, Pittsburgh, PA). Unbiased stereology in Fig. 3 was carried out as previously reported (De Miranda et al., 2018; Tapias et al., 2013; Zharikov et al., 2015). One in every six midbrain sections was immunolabeled for TH and co-labeled with DAPI and NeuroTrace 640/660 fluorescent Nissl dye (Invitrogen, Carlsbad, CA). Images were acquired using an automated Nikon 90i upright microscope with a 20× objective (NA = 0.75), equipped with a linear-encoded motorized stage and Q-imaging Retiga cooled CCD camera. Micrographs were analyzed

Table 1
Primary antibodies used in this study.

Antigen	Vendor	Catalogue #	Species	Figure	Dilution
α-Synuclein	BD Biosciences	610787	Mouse	4 (IF)	1:3000
Tyrosine hydroxylase	Millipore	Ab1542	Rabbit	3, 4 (IF)	1:2000
	Millipore	MAB 318	Mouse	2 (IHC)	1:2000
GFP	Abcam	Ab6673	Goat	3, 4 (IF)	1:4000
	Millipore	MAB 3580	Mouse	2 (IHC)	1:4000
GFAP	Cell Signaling	3670	Mouse	3 (IF)	1:1000
IBA-1	Wako	019-19741	Rabbit	3 (IF)	1:1000
DAT	Thermo Fisher	MA5-24796	Mouse	3 (IF)	1:500

using NIS-Elements Advanced Research software (Nikon, Melville, NY). A region of interest was drawn around the substantia nigra pars compacta and neurons were quantified by a single investigator blinded to experimental group. The software counted all cells in which Nissl and DAPI ($Nissl^+$) or Nissl, DAPI and TH (TH^+) coincided. The method yields identical results to manual stereology, but has a lower coefficient of error owing to the greater number of neurons sampled (Tapias and Greenamyre, 2014; Tapias et al., 2013). Quantification of α-synuclein expression in Fig. 4 was carried out using an Olympus FV-1000 confocal microscope (B + B Microscopes, Pittsburgh, PA), with constant laser and detector settings that were optimized to avoid saturation in the α-synuclein and TH channels. Regions of interest were drawn around at least 300 dopaminergic (TH^+) neurons on 4–6 sections from each side of each animal, allowing measurement of mean α-synuclein immunofluorescence within each ROI using Fluoview software (Olympus, B + B Microscopes, Pittsburgh, PA). Pseudocoloring images and Boolean operations were carried out using Fluoview software. Dopaminergic terminal density in the striatum was determined by measuring tyrosine hydroxylase immunofluorescence as previously described (De Miranda et al., 2018; Zharikov et al., 2015). Forebrain sections labeled with anti-TH primary was incubated with a secondary antibody conjugated to LI-COR IRDye 680 or 800CW. Sections were imaged using a LICOR infrared scanner with a wide linear measurement range. Identically-sized regions of interest were drawn within in the striatum on each side and mean fluorescence intensity measured using LiCOR software.

2.4. RNA in situ hybridization

A digoxigenin-labeled cRNA probe to *Snca* mRNA was generated by *in vitro* transcription as previously described (Zharikov et al., 2015). Brain sections were washed in PBS, treated with 0.1% DEPC in PBS for 15 min × 2, equilibrated in 5 x SSC, post-fixed in 4% PFA and washed in PBS. Sections were then incubated in UltraHyb (Ambion, Austin, TX) supplemented with 1 mg/mL Torula RNA (Sigma, St. Louis, MO) for one hour at 68 °C. Probe was then added to a final concentration of 150 ng/mL and hybridized at 68 °C overnight. Hybridization buffer and unbound probe were removed by washing in 2 x SSC; stringency washes were carried out at 68 °C in 0.1 x SSC. Hybridized probe was localized using alkaline phosphatase (AP)-conjugated anti-digoxigenin antibody (Roche, Indianapolis, IN) and bound antibody detected by a histochemical reaction using an AP substrate (BM Purple, Roche). $Snca^+$ cell counts were made on both sides of the midbrain in three sections per animal in a region of interest defined by TH immunoreactivity on the adjacent section.

2.5. Statistical analysis

Data were analyzed using the following statistical tests: Fig. 1B, C: 2-way ANOVA, with time and experimental group as variables; Figs. 2C, D, 1-way ANOVA with Tukey's *post hoc* test to compare 4 groups (2-tailed paired *t*-test comparing the two sides of the same sections yielded similar results); Figs. 3A, B, F, H, 4D, 2-tailed unpaired *t*-test with correction for unequal variance.

3. Results

In order to investigate the consequences of long-term α-synuclein knockdown in the adult CNS *in vivo*, we employed our previously-reported RNA interference vector AAV-sh[Snca] (Zharikov et al., 2015). We have previously shown that this vector specifically targets rat *Snca* mRNA (encoding α-synuclein) *in vivo*, without causing toxicity at 3 or 6 weeks post-transduction (Zharikov et al., 2015). The control vector AAV-sh[Ctrl] is isogenic, with the exception that the *Snca* shRNA sequence is replaced by a non-targeting control shRNA. Animals underwent unilateral vector inoculation with a single infusion immediately dorsal to the substantia nigra. Since we were predominantly interested in potential toxicity, we employed a higher vector dose than used in our previous studies (6.68×10^9 genome copies/infusion site compared with 4×10^9 used by Zharikov et al., 2015).

Rats were monitored clinically for 1 year after vector infusion surgery (the experimental time course is shown in Fig. 1A), with weekly measurement of weight, evaluation of forelimb function using a postural instability test that is sensitive to nigrostriatal function (Woodlee et al., 2008; Zharikov et al., 2015), observation of behavior, and general physical examination during regular handling. No overt clinical abnormalities were apparent in either experimental group for the 52 weeks following vector inoculation. Animals that received either AAV-sh[Snca] or AAV-sh[Ctrl] ate a normal diet and showed steady weight gain, eventually approaching a 50% increase from their baseline weight over the 52 weeks following vector inoculation (Fig. 1B). There was a trend towards marginally increased weight gain in the AAV-sh[Snca] group, but this was not statistically significant (Fig. 1B - the y-axis is expanded to illustrate the small difference). No clinical motor asymmetry was observed at any point during regular handling, or while rats were behaving spontaneously in their cages. Forelimb motor function was symmetric in both experimental groups throughout the period of clinical monitoring and there was no evidence of impaired nigrostriatal function as evaluated by the postural instability test (Fig. 1C). The inset panel in fig. 1C shows data redrawn from our prior study (Zharikov et al., 2015) for comparison; these previously reported data illustrate the large unilateral change that can be detected in this assay in the presence of asymmetrically impaired nigrostriatal function. Together, our new data show that intranigral inoculation with either AAV-sh[Snca] or AAV-sh[Ctrl] did not lead to detectable clinical phenotypes over one year of post-procedure observation.

52 weeks after vector inoculation, brain tissue was fixed for histological analysis. Adjacent midbrain sections were labeled for tyrosine hydroxylase (TH) by immunohistochemistry and *Snca* mRNA by *in situ* hybridization (Figs. 2A and B). Similar TH immunoreactivity was seen on the two sides of midbrain sections from all animals (upper panels of Fig. 2A and B) showing that the substantia nigra was intact after vector inoculation, regardless of vector genotype. The *Snca* mRNA signal was dramatically decreased in the substantia nigra after AAV-sh[Snca] transduction (Fig. 2A, lower panels), but unchanged after transduction with AAV-sh[Ctrl] (Fig. 2B, lower panels). We counted cells expressing *Snca* mRNA (Fig. 2C) manually and quantified the strength of the *Snca* ISH signal by densitometry (Fig. 2D). Overall there was ≈ 90% decrease in the number of *Snca*-expressing nigral cells ($p < .0001$) and ≈ 85% decrease in the *Snca* ISH signal ($p = .0005$) in the substantia nigra that received AAV-sh[Snca] compared with control side of the same sections (1-way ANOVA with Tukey's *post hoc* test). There were no significant differences between the AAV-sh[Ctrl] transduced and control sides of the same sections, or between the control sides of AAV-sh[Snca] and AAV-sh[Ctrl] animals. To test whether these *Snca* mRNA expression differences could be attributable to persistent vector transgene expression, we labeled tissue for GFP, which is co-expressed with shRNA in both AAV-sh[Snca] and AAV-sh[Ctrl] (Fig. 2E). Robust GFP expression was evident in tissue from all animals, in the ventral midbrain around the substantia nigra and along the trajectory through which the needle entered the brain during inoculation. GFP immunoreactivity was also evident in the striatum ipsilateral to vector inoculation, indicating expression within transduced dopaminergic nigrostriatal neurons. No GFP expression was seen contralateral to inoculation, either in the midbrain or forebrain. Together, these data show that, 52 weeks after vector inoculation, the substantia nigra receiving AAV-sh[Snca] was grossly intact and showed ongoing vector transgene expression, resulting in significantly attenuated *Snca* mRNA expression in transduced neurons.

We next evaluated the integrity of the substantia nigra in more detail (Fig. 3). Unbiased stereology was employed to quantify the number of Nissl-labeled neurons within the substantia nigra on each side of the brain. There were no significant differences between the

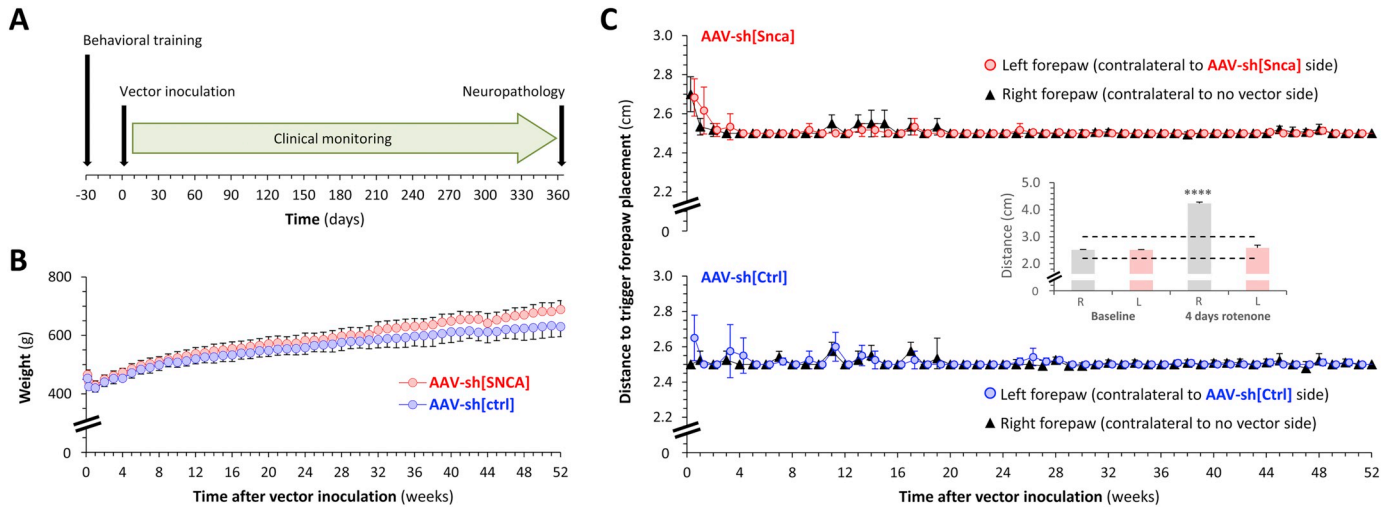

Fig. 1. No clinical phenotype in adult rats over the 52 weeks following unilateral inoculation of AAV-sh[Snca] into the substantia nigra. A: Experimental design. All time points are relative to day of intracerebral vector inoculation (day 0). B: Mean ± SE weight (g) of rats over the 52 weeks following inoculation with AAV-sh [Snca] (red, $n = 5$) or AAV-sh[Ctrl] (blue, $n = 4$). Note truncated y-axis. C: The postural instability test was used to evaluate nigrostriatal function. Graphs show mean ± SE displacement necessary to trigger forepaw placement over the 52 weeks following inoculation with AAV-sh[Snca] (red, upper graph, n = 5) or AAV-sh [Ctrl] (blue, lower graph, $n = 4$). Note truncated y-axes. For each experimental group, data are superimposed for the negative control right forepaw (ipsilateral to vector inoculation; black triangles) and left forepaw (contralateral to vector inoculation; colored circles). The inset panel shows data redrawn from our prior publication (Zharikov et al., 2015) to illustrate the large unilateral increase in trigger distance that can be detected using this method in the setting of unilateral nigrostriatal dysfunction. In this case the motor deficit was induced by 4 days of rotenone exposure, with the asymmetry arising from neuroprotection following unilateral α-synuclein knockdown (red bars). The dotted lines in the inset graph show the y-axis limits for the main panel. Data analysis in panels B and C was performed by 2-way ANOVA. There were no significant differences between treatment groups (B, C) or sides (C) at any time point.

number of Nissl$^+$ neurons on the vector-transduced and control sides of the brain in either experimental group (control side 11,664 ± 2836 *versus* AAV-sh[Snca] side 11,118 ± 3038, $p = .99$; control side 11,853 ± 951 *versus* AAV-sh[Ctrl] side 9858 ± 666, $p = .91$; 1-way ANOVA with Tukey's *post hoc* test). In order to compare more directly the effect of the two vectors on neuronal viability, the number of Nissl$^+$ neurons on the vector-transduced side of the brain was expressed as % of the control side for each animal (Fig. 3A). There was no difference between AAV-sh[Snca] and AAV-sh[Ctrl] in the number of Nissl$^+$ neurons on the vector-transduced side relative to the control side (AAV-sh[Snca] 92.5 ± 7% *versus* AAV-sh[Ctrl] 83.6 ± 3%, $p = .3$, unpaired *t*-test). Overall, these data show that neither vector caused significant neurodegeneration.

To evaluate the neurochemical phenotype of the surviving cells, we next quantified the number of TH-expressing neurons within the substantia nigra on each side of the brain by unbiased stereology. There was a non-significant trend towards a decrease in the number of TH-expressing neurons on the transduced side of the substantia nigra, regardless of vector genotype (control side 10,713 ± 2851, *versus* AAV-sh[Snca] side 7757 ± 2411, $p = .73$; control side 8636 ± 1029 *versus* AAV-sh[Ctrl] side 5985 ± 1077, $p = .79$; 1-way ANOVA with Tukey's *post hoc* test). Expressing the number of TH$^+$ neurons on the vector-transduced side relative to control (Fig. 3B) to allow direct comparison between experimental groups showed no difference between the two vectors (AAV-sh[Snca] 69.94 ± 13%, *versus* AAV-sh[Ctrl] 69.62 ± 11%, $p = .99$, unpaired *t*-test). Overall, these data suggest that TH expression was decreased in the substantia nigra 12 months following transduction with either control vector or α-synuclein-targeting vector.

Localized, severe loss of TH expression was apparent in the substantia nigra immediately adjacent to the inoculation sites of both vectors (Fig. 3C). On adjacent sections, a large and spatially-restricted increase in the number of GFAP-expressing astrocytes was noted near the infusion site, suggesting the presence of gliosis (Fig. 3D, left panels). However, there was no change in the abundance or morphology of IBA1-expressing microglia, either near the infusion site (Fig. 3D, right panels) or in the vicinity of GFP-expressing transduced cells distant from the infusion site. These findings were identical after exposure to either vector, showing that astrogliosis was not caused by α-synuclein knockdown.

Since pathology in degenerating neurons can start in the distal axon, we evaluated the density of striatal dopaminergic terminals in forebrain samples from the same animals, using quantitative near-infrared immunofluorescence to measure immunoreactivity for TH (Fig. 3E – F) and DAT (Fig. 3G – H). There was no overt asymmetry in TH or DAT expression at any level of the striatum in either experimental group (Fig. 3E, G). Quantification showed a non-significant trend towards a modest reduction in striatal TH expression on the vector-transduced side of both groups (control side 543 ± 45 units *versus* AAV-sh[Snca] side 470 ± 27 units, $p = .69$; control side 752 ± 151 units *versus* AAV-sh[Ctrl] side 618 ± 82 units, $p = .90$; 1-way ANOVA with Tukey's *post hoc* test). There was no difference in striatal DAT expression on the vector-transduced side compared with the control side in either group (control side 1003 ± 145 units *versus* AAV-sh[Snca] side 966 ± 98 units, p = .99; control side 908 ± 61 units *versus* AAV-sh [Ctrl] side 849 ± 41 units, $p = .96$; 1-way ANOVA with Tukey's *post hoc* test). By expressing immunofluorescence signal on the vector-transduced side of the brain as % of the no-vector side to facilitate comparison (Fig. 3F), both vectors were shown to influence striatal expression of TH (AAV-sh[Snca] 85 ± 5% *versus* AAV-sh[Ctrl] 86 ± 8%, $p = .95$, unpaired *t*-test) and DAT (Fig. 3H; AAV-sh[Snca] 95 ± 4% *versus* AAV-sh[Ctrl] 98 ± 5%, $p = .61$, unpaired *t*-test) similarly.

Finally, we quantified α-synuclein expression in animals receiving either AAV-sh[Snca] or AAV-sh[Ctrl] (Fig. 4), using confocal microscopy to measure α-synuclein immunoreactivity within dopaminergic neurons. Fig. 4A shows example confocal planes of the substantia nigra on each side of the same sections, from animals receiving each vector. GFP (green; upper panels) expression was apparent on the vector-transduced side of animals in both experimental groups, and showed substantial overlap with TH (red; middle panels) in dopaminergic neurons. α-Synuclein (white; lower panels) expression was seen within dopaminergic neurons transduced with AAV-sh[Ctrl] but not within neurons transduced with AAV-sh[Snca]. The striking reduction in nigral

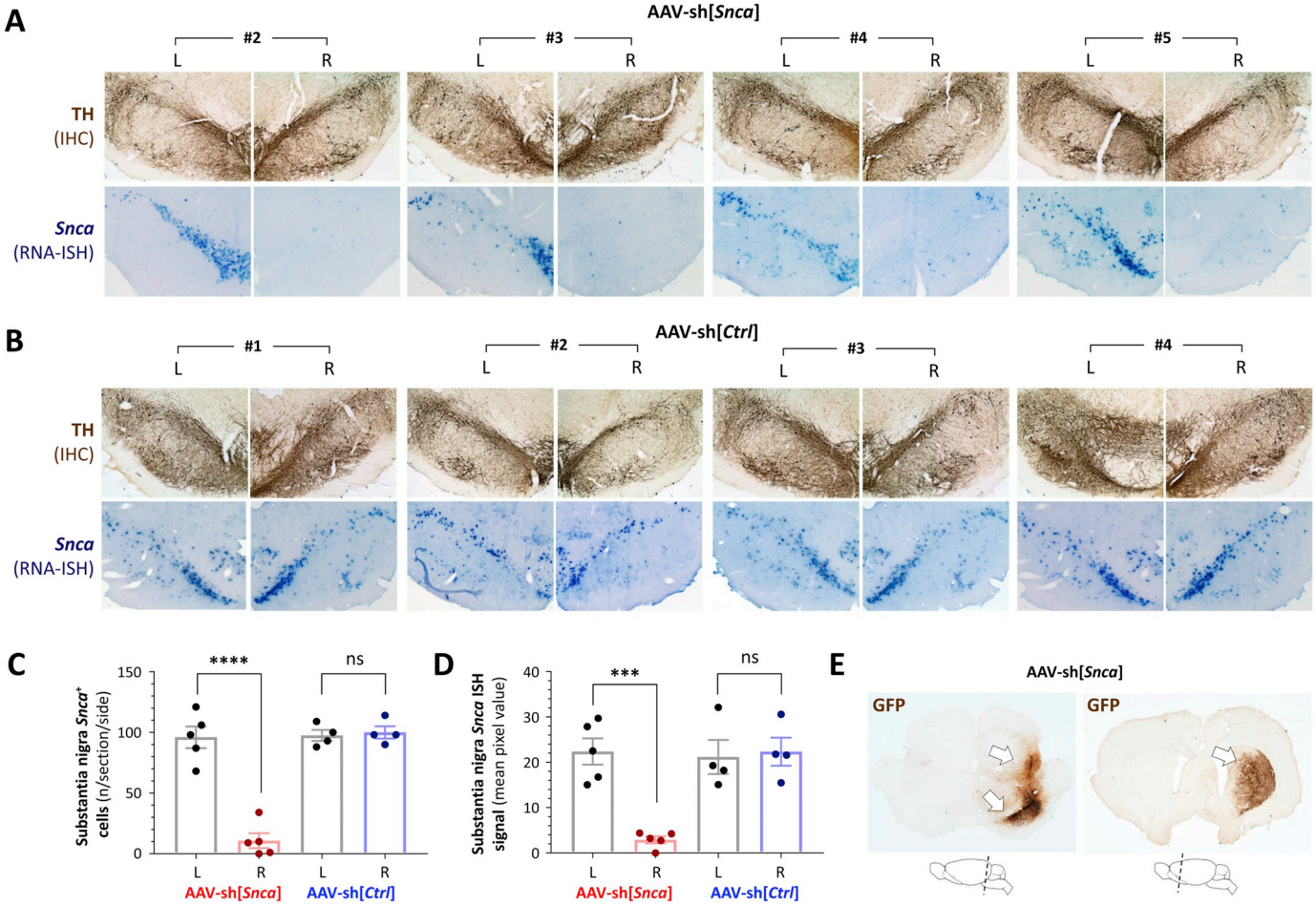

Fig. 2. Loss of *Snca* mRNA expression in the substantia nigra and persistent transgene expression 52 weeks after AAV-sh[*Snca*] inoculation. A: Photomicrographs of the substantia nigra are shown for animals #2 – #5 in the group receiving AAV-sh[*Snca*]. Each pair of images shows the substantia nigra on each side (labeled L and R) of the same section. Top row: immunohistochemistry (IHC) for tyrosine hydroxylase (TH; brown) showing the position and integrity of the substantia nigra. Bottom row: RNA *in situ* hybridization (ISH) for the *Snca* mRNA transcript (purple). IHC and ISH were performed on adjacent sections. B: Similar to panel A, showing sections from each animal in the group receiving AAV-sh[Ctrl]. Top row: IHC for TH (brown). Bottom row: RNA ISH for the *Snca* mRNA transcript (purple). C: The number of *Snca* mRNA-expressing cells was counted on each side of the substantia nigra for three sections per animal. Individual data points show the mean value for each animal (AAV-sh[*Snca*] $n = 5$; AAV-sh[Ctrl] $n = 4$) and side; bars show the group mean ± 95% CI. D: The *Snca* mRNA ISH signal was quantified by densitometry in the region corresponding to the substantia nigra on each side of three midbrain sections per animal. Individual data points show the mean value for each animal and side; bars show the group mean ± 95% CI. E: Expression of the vector-encoded GFP transgene was determined in the midbrain (left) and forebrain (right) by IHC for GFP (brown), demonstrating persistent presence and expression of the AAV vector 52 weeks post-transduction. The cartoons below the micrographs indicate the planes of the sections shown. Panels C and D were analyzed by 1-way ANOVA with Tukey's *post hoc* test. ***$p < .0001$, ****$p < .00001$.

α-synuclein immunoreactivity on the AAV-sh[Snca] side of the brain was further illustrated using a color intensity scale (Fig. 4B), and the loss of α-synuclein signal from within dopaminergic neurons was illustrated using a Boolean *AND* function to show areas of the image that were immunoreactive for both TH and α-synuclein (Fig. 4C). Using the TH channel to define regions of interest corresponding to dopaminergic neurons in multiple sections from each animal, we quantified the signal in the α-synuclein channel while blinded to the α-synuclein image (Figs. 4D – F). Scatter plots (Fig. 4E) showed an obvious and very large decrease in α-synuclein signal within dopaminergic neurons on the AAV-sh[Snca] transduced side of the substantia nigra relative to the control no-vector side (Fig. 4E). A modest decrease in α-synuclein immunoreactivity was also observed on the AAV-sh[Ctrl] transduced side of the brain relative to the no-vector side (Fig. 4F). Expressed as % of the no-vector side (Fig. 4D), dopaminergic neuronal α-synuclein expression was decreased significantly more in animals that received AAV-[Snca] (73 ± 1.2% decrease) than AAV-sh[Ctrl] (24 ± 5% decrease, $p = .001$, unpaired *t*-test).

Together, these data show evidence of mild non-specific toxicity in both experimental groups, presumably attributable to a combination of vector inoculation surgery, cellular transduction and transgene expression. However, robust α-synuclein knockdown was measured in > 2000 apparently healthy substantia nigra dopaminergic neurons 12 months after vector transduction. In the absence of demonstrable cell loss, these data show unequivocally that long-term suppression of α-synuclein expression in the adult brain does not cause neurodegeneration.

4. Discussion

These data are important in the context of ongoing attempts to develop PD therapeutics that target α-synuclein expression. Since PD is a chronic disease, it is likely that prolonged therapeutic knockdown of α-synuclein expression would be necessary to impact pathogenesis. The effects of endogenous α-synuclein knockdown in the adult brain, for longer than a few weeks, have not been reported. Our data show that adult substantia nigra dopaminergic neurons tolerate > 70% reduction in α-synuclein expression for 12 months, which is approximately half of the lifespan of a rat.

Our study design included an isogenic control vector that carries a

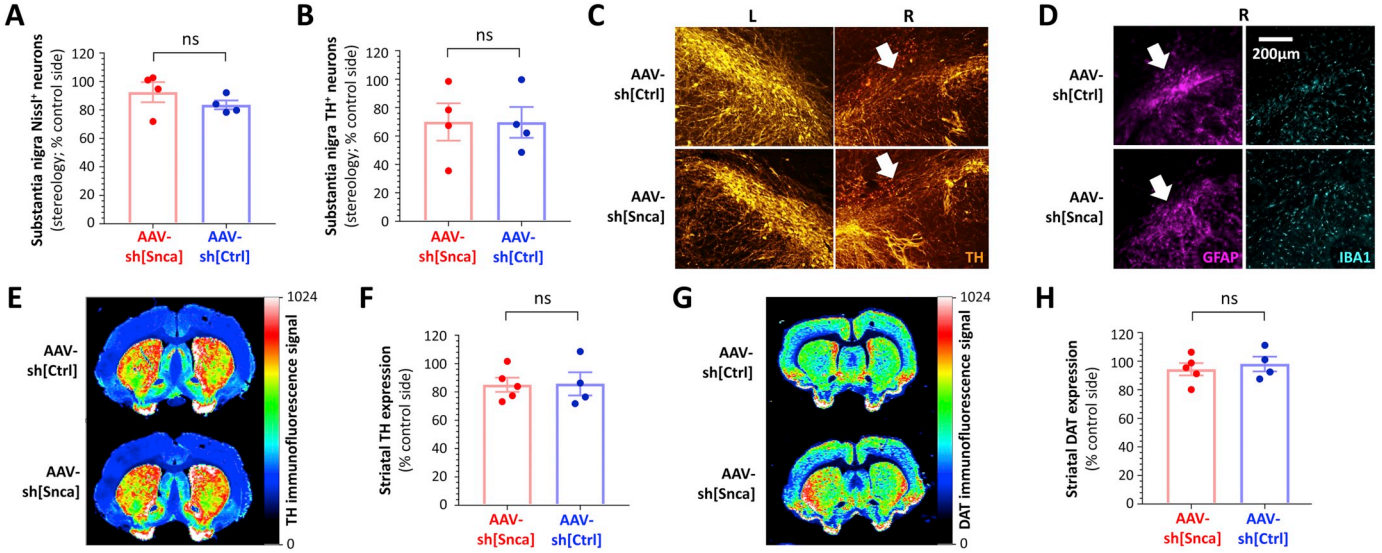

Fig. 3. Absence of neurodegeneration but decreased TH expression and astrogliosis in the substantia nigra 52 weeks after inoculation with either AAV-sh[Snca] or AAV-sh[Ctrl]. A: Unbiased stereology was used to quantify Nissl$^+$ neurons on each side of the substantia nigra from rats that received AAV-sh[Snca] (red, left, n = 4) or AAV-sh[Ctrl] (blue, right, n = 4). Data points show values for individual animals, expressed as % of the control non-transduced side in the same animal. Bars show group mean ± SE. B: Unbiased stereology was used to quantify TH$^+$ neurons on each side of the substantia nigra from rats that received AAV-sh[*Snca*] (red, left, n = 4) or AAV-sh[Ctrl] (blue, right, n = 4). Data points show values for individual animals, expressed as % of the control non-transduced side in the same animal. Bars show group mean ± SE. C: Epifluorescence micrographs of the substantia nigra at the point of vector delivery, labeled for TH (orange). Localized loss of TH-expressing cells following delivery of either AAV-sh[Ctrl] (upper row) or AAV-sh[Snca] (lower row) is indicated by white arrows. D: Epifluorescence micrographs of the substantia nigra in adjacent sections to panel C, labeled for GFAP (magenta, left) and IBA-1 (cyan, right). Localized astrogliosis at the site of vector inoculation following delivery of either AAV-sh[Ctrl] (upper row) or AAV-sh[Snca] (lower row) is indicated by white arrows. E – H: Quantitative near-infrared immunofluorescence was employed to quantify TH (E, F) and DAT (G, H) expression in the striatum. E and G show forebrain sections from animals inoculated with AAV-sh[Ctrl] (top) or AAV-sh[Snca] (bottom). The intensity of immunoreactivity is depicted using the color scale shown to the right of each panel. Immunoreactivity for TH (F) and DAT (H) was quantified on each side of the striatum, from rats that received AAV-sh[*Snca*] (red, left, n = 5) or AAV-sh[Ctrl] (blue, right, n = 4). Data points show values for individual animals (mean of 5 sections for each animal) expressed as % of the control non-transduced side for the same animal. Bars show group mean ± SE. Data were analyzed by unpaired 2-tailed *t*-tests. There were no significant differences between vectors.

non-targeting shRNA, for comparison with the α-synuclein knockdown vector. In view of the inherent variability of vector preparations, we were careful to generate the two vectors in parallel at every stage, from streaking glycerol plasmid stocks, through to the final purification of vector particles. This ensured, as far as possible, that any differences between the two vector stocks in parameters such as titer, non-packaged DNA, and transduction-deficient particles, were minimized. Since the vector stocks consequently differed only in their shRNA sequences, we were able to distinguish changes attributable to vector exposure from those attributable to shRNA targeting the *Snca* mRNA transcript. The only endpoint that differed significantly between the two experimental groups was the substantially decreased *Snca* mRNA and α-synuclein expression that we observed in the substantia nigra of animals that received AAV-sh[*Snca*]. In contrast, non-specific toxicities attributable to vector exposure – including loss of TH expression in 30% substantia nigra neurons, damage to the substantia nigra and astrogliosis immediately surrounding the vector infusion site – were identical in both experimental groups.

The mechanisms of vector-mediated toxicity are likely to include mechanical effects of intra-mesencephalic infusion, low levels of impurities in the vector preparations, cellular toxicity or immunogenicity from the GFP reporter gene (Ansari et al., 2016), and effects of robust shRNA expression, independent of gene targeting. Toxicity from shRNA *in vivo* is well-recognized and has been characterized in the liver, where it was shown that highly-expressed exogenous shRNAs and essential cellular miRNAs compete for a shared nuclear export mechanism dependent on exportin-5 (Grimm et al., 2006). Non-specific toxicity resulting from viral shRNA delivery also occurs in the CNS (McBride et al., 2008; Ulusoy et al., 2009). In a study targeting TH in the adult rat substantia nigra (Ulusoy et al., 2009), loss of VMAT-immunoreactive neurons (indicating degeneration of dopaminergic neurons, or downregulation of a non-targeted gene) was seen even in the absence of shRNA at high doses of vector ($> 5 \times 10^9$ GC/site). Additional toxicity attributable to shRNA was apparent at considerably lower doses, necessitating vector doses below 5×10^8 GC/site to eliminate non-specific toxicity for some constructs. In another study, selected shRNA sequences targeting the mRNA encoding Huntingtin provoked neuroinflammation and loss of DARPP32 immunoreactivity in the striatum. Similar toxicity was seen with control scrambled shRNA sequences, and was found to correlate with the expression levels of the shRNA (McBride et al., 2008). Adverse effects of shRNA can be mitigated by using shorter shRNA sequences (Grimm et al., 2006), or by reducing shRNA expression levels. The latter can be accomplished by using a Pol-II promoter (Giering et al., 2008) instead of the Pol-III promoters commonly used to over-express short RNAs (Makinen et al., 2006), or by using a lower vector dose (Ulusoy et al., 2009). This may account for the lack of non-specific toxicity seen in our prior study, in which we used 40% lower vector dose than the present study (Zharikov et al., 2015). Alternatives to viral shRNA delivery are currently under development for therapeutic gene targeting in the CNS *in vivo*. These include synthetic miRNAs (Borel et al., 2016; Evers et al., 2018; Han et al., 2011), antisense oligonucleotides (Scoles et al., 2017), and deployment of monoclonal antibodies against relevant protein targets (Castillo-Carranza et al., 2015). It is unclear at this point which modality will be safest, most effective, and practicable in a clinical setting. However, the availability of means to mitigate shRNA toxicity and alternative approaches to virally-delivered shRNA suggests that shRNA toxicity should not itself be an insurmountable barrier to therapeutic down-regulation of α-synuclein in PD.

We estimated *Snca* mRNA knockdown at 12 months to be approximately 90%. This is likely an over-estimate, because of the non-linear relationship between mRNA expression level and chromogenic ISH

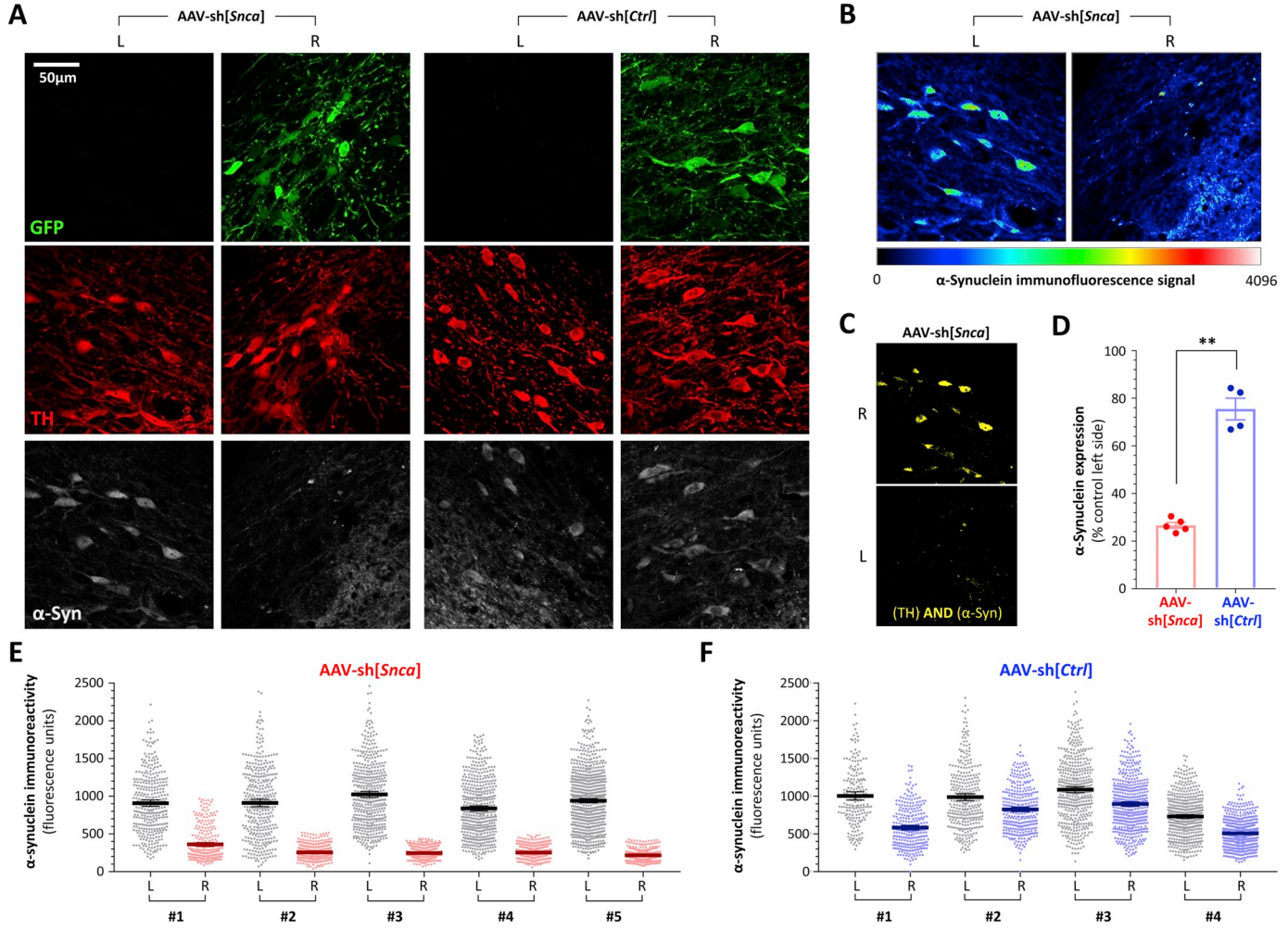

Fig. 4. Persistent loss of α-synuclein expression in TH-expressing nigral dopaminergic neurons, 52 weeks after inoculation with AAV-sh[*Snca*]. A: Confocal planes of the substantia nigra on each side of the same midbrain sections are shown from animals inoculated with AAV-sh[*Snca*] (left) or AAV-sh[Ctrl] (right). The sections were immunolabeled for GFP (green), TH(red), α-synuclein (white). The scale bar for all 12 images is shown in the top left image. Images from the AAV-sh[Snca] inoculated animal are further analyzed in panels B and C. B: α-Synuclein immunoreactivity is illustrated using a color intensity scale (shown beneath the images) to demonstrate the loss of α-synuclein expression in nigral dopaminergic neurons that received AAV-sh[Snca]. C: A Boolean *AND* operation was employed to identify pixels from the same confocal plane that showed both TH and α-synuclein immunoreactivity. The resulting image further illustrates loss of α-synuclein expression in dopaminergic neurons 52 weeks after AAV-sh[Snca] inoculation. D, E, F: The TH channel was used to define regions of interest in confocal planes from both sides of multiple midbrain sections, thereby allowing blinded quantification of α-synuclein expression within 350–700 dopaminergic neurons from each side of each animal. (E) and (F) show scatter plots of α-synuclein immunoreactivity in individual cells from the control and vector sides of animals inoculated with (E) AAV-sh[Snca] or (F) AAV-sh[Ctrl]; bars show mean and 95% CI. (D) shows the mean for each animal expressed as % of the control non-transduced side. Panel D was analyzed using unpaired 2-tailed *t*-test, $^{**}p < .01$ AAV-sh[Snca] *vs* AAV-sh[Ctrl].

signal relative to background at low expression levels. We estimated α-synuclein protein knockdown to be approximately 70%. This is likely an under-estimate, because we measured α-synuclein expression in all TH^+ cells, regardless of whether GFP expression was present. Consequently, the sample includes a contribution from the small proportion of dopaminergic neurons that were not transduced by the vector, and these cells may have retained baseline α-synuclein expression. In view of these considerations, we estimate α-synuclein knockdown at 12 months to be at least 70% and probably higher. We intentionally quantified α-synuclein expression only in TH^+ cells, to determine the degree of α-synuclein knockdown in dopaminergic neurons that had retained their neurochemical phenotype. Overall, a large number of healthy nigral dopaminergic neurons tolerated robust α-synuclein knockdown for a year. We conclude that > 70% long-term reduction in α-synuclein expression does not cause neurodegeneration.

Our present findings are in line with multiple other studies reporting the absence of neurodegeneration following knockdown of endogenous α-synuclein in the adult CNS (Alarcon-Aris et al., 2018; Cooper et al., 2014; Helmschrodt et al., 2017; McCormack et al., 2010; Zharikov et al., 2015) or in $Snca^{-/-}$ mice (Abeliovich et al., 2000; Cabin et al., 2002). In contrast, two previous publications (Benskey et al., 2018; Gorbatyuk et al., 2010) reported acute loss of dopaminergic neurons after intranigral inoculation of AAV-shRNA vectors targeting *Snca*. Partial rescue of cell loss in $Snca^{-/-}$ mice was presented as evidence that neurodegeneration was attributable to acute loss of α-synuclein in WT rats exposed to the vectors (Benskey et al., 2018). Since our prior study reported 30–40% reduction in nigral α-synuclein expression without toxicity (Zharikov et al., 2015), compared with 86% (Gorbatyuk et al., 2010) and 57% (Benskey et al., 2018) decrease in the studies showing neurodegeneration, it was suggested that the amount of α-synuclein knockdown might be a critical factor contributing to cell loss (Benskey et al., 2018). However, our current study shows > 70% α-synuclein knockdown without neurodegeneration. Consequently, the expression level of α-synuclein cannot be the only explanation for the observed toxicity in the prior studies. Other factors, such as the rate of decrease of α-synuclein expression, or technical issues unrelated to α-synuclein expression, may be important.

There are several methodological differences between our studies on α-synuclein knockdown and the publications showing neurodegeneration. Our vectors are AAV2-based (Zharikov et al., 2015), whereas the vectors causing neurodegeneration are AAV2/5 pseudotypes (Benskey et al., 2018; Gorbatyuk et al., 2010). AAV5-pseudotyped vectors are not thought to exhibit neuron-specific tropism and there is concern that transduction of antigen presenting cells by vectors with wider tropism than AAV2 could trigger an immune response (Ciesielska et al., 2013; Howard et al., 2008). This may be relevant, given the proposed central role of inflammation in the cell death observed after AAV2/5 shRNA α-synuclein knockdown in the substantia nigra (Benskey et al., 2018). The shRNA sequences in our vectors are non-overlapping with the sequences reported to cause toxicity. As discussed above, it is well-recognized that shRNA sequence can alter non-specific toxicity profoundly in the substantia nigra (Ulusoy et al., 2009). Our studies employed 6–8 month old male Lewis rats (Zharikov et al., 2015) whereas Sprague-Dawley rats (Benskey et al., 2018) were used in the studies showing neurodegeneration; experimental outcomes in neurobiology are well known to be sensitive to animal strain. Further differences between the studies include the vector doses and infusion rates (4×10^9 GC or 6.8×10^9 GC in 2 μL at 0.2 μL/min per site in our studies, *versus* 3.9×10^9 GC in 1.5 μL at 0.5 μL/min per site (Benskey et al., 2018; Gorbatyuk et al., 2010)) and the Pol-III promoters used to express shRNA (U6 in our vectors, H1 in the vectors causing cell loss (Benskey et al., 2018; Gorbatyuk et al., 2010)). It is unclear whether any of these factors explains the different outcomes in these studies. However, given the numerous sources of experimental variability inherent in viral shRNA knockdown in the CNS, it would seem advisable for future experiments to exploit alternative methods – such as conditional knockout mice or oligonucleotide delivery – to resolve questions such as the influence of the rate of decline of α-synuclein levels on neuronal health.

Our present study demonstrates unequivocally that α-synuclein expression can be reduced robustly and for prolonged periods of time within the adult substantia nigra without causing neurodegeneration. Given the central role of α-synuclein in PD and growing interest in the development of therapies directed at modulating α-synuclein expression, these are important findings with translational implications.

Acknowledgements

This work was supported by research grants from NINDS (ES022644, NS095387), the US Department of Veterans Affairs (BX000548), The Blechman Foundation, the American Parkinson Disease Association (Center for Advanced Research), and the University of Pittsburgh Medical Center. We gratefully acknowledge technical assistance from Matthew T. Keeney. This article does not represent the views of the US government.

References

Abeliovich, A., et al., 2000. Mice lacking alpha-synuclein display functional deficits in the nigrostriatal dopamine system. Neuron 25, 239–252.
Alarcon-Aris, D., et al., 2018. Selective alpha-synuclein knockdown in monoamine neurons by intranasal oligonucleotide delivery: potential therapy for Parkinson's disease. Mol. Ther. 26, 550–567.
Ansari, A.M., et al., 2016. Cellular GFP toxicity and immunogenicity: potential confounders in in vivo cell tracking experiments. Stem Cell Rev. 12, 553–559.
Benskey, M.J., et al., 2018. Silencing alpha synuclein in mature nigral neurons results in rapid neuroinflammation and subsequent toxicity. Front. Mol. Neurosci. 11, 36.
Betarbet, R., et al., 2000. Chronic systemic pesticide exposure reproduces features of Parkinson's disease. Nat. Neurosci. 3, 1301–1306.
Borel, F., et al., 2016. Therapeutic rAAVrh10 mediated SOD1 silencing in adult SOD1(G93A) mice and nonhuman primates. Hum. Gene Ther. 27, 19–31.
Cabin, D.E., et al., 2002. Synaptic vesicle depletion correlates with attenuated synaptic responses to prolonged repetitive stimulation in mice lacking alpha-synuclein. J. Neurosci. 22, 8797–8807.
Cannon, J.R., et al., 2009. A highly reproducible rotenone model of Parkinson's disease. Neurobiol. Dis. 34, 279–290.
Castillo-Carranza, D.L., et al., 2015. Tau immunotherapy modulates both pathological tau and upstream amyloid pathology in an Alzheimer's disease mouse model. J. Neurosci. 35, 4857–4868.
Chartier-Harlin, M.C., et al., 2004. Alpha-synuclein locus duplication as a cause of familial Parkinson's disease. Lancet 364, 1167–1169.
Ciesielska, A., et al., 2013. Cerebral infusion of AAV9 vector-encoding non-self proteins can elicit cell-mediated immune responses. Mol. Ther. 21, 158–166.
Cooper, J.M., et al., 2014. Systemic exosomal siRNA delivery reduced alpha-synuclein aggregates in brains of transgenic mice. Mov. Disord. 29, 1476–1485.
Cronin, K.D., et al., 2009. Expansion of the Parkinson disease-associated SNCA-Rep1 allele upregulates human alpha-synuclein in transgenic mouse brain. Hum. Mol. Genet. 18, 3274–3285.
Dauer, W., et al., 2002. Resistance of alpha -synuclein null mice to the parkinsonian neurotoxin MPTP. Proc. Natl. Acad. Sci. U. S. A. 99, 14524–14529.
De Miranda, B.R., et al., 2018. Astrocyte-specific DJ-1 overexpression protects against rotenone-induced neurotoxicity in a rat model of Parkinson's disease. Neurobiol. Dis. 115, 101–114.
Edwards, T.L., et al., 2010. Genome-wide association study confirms SNPs in SNCA and the MAPT region as common risk factors for Parkinson disease. Ann. Hum. Genet. 74, 97–109.
Evers, M.M., et al., 2018. AAV5-miHTT Gene therapy demonstrates broad distribution and strong human mutant huntingtin lowering in a Huntington's disease minipig model. Mol. Ther. 26 (9), 2163–2177.
Fornai, F., et al., 2005. Parkinson-like syndrome induced by continuous MPTP infusion: convergent roles of the ubiquitin-proteasome system and alpha-synuclein. Proc. Natl. Acad. Sci. U. S. A. 102, 3413–3418.
Fuchs, J., et al., 2008. Genetic variability in the SNCA gene influences alpha-synuclein levels in the blood and brain. FASEB J. 22, 1327–1334.
Giering, J.C., et al., 2008. Expression of shRNA from a tissue-specific pol II promoter is an effective and safe RNAi therapeutic. Mol. Ther. 16, 1630–1636.
Gorbatyuk, O.S., et al., 2010. In vivo RNAi-mediated alpha-synuclein silencing induces nigrostriatal degeneration. Mol. Ther. 18, 1450–1457.
Grimm, D., et al., 2006. Fatality in mice due to oversaturation of cellular microRNA/short hairpin RNA pathways. Nature 441, 537–541.
Han, Y., et al., 2011. A microRNA embedded AAV alpha-synuclein gene silencing vector for dopaminergic neurons. Brain Res. 1386, 15–24.
Helmschrodt, C., et al., 2017. Polyethylenimine Nanoparticle-Mediated siRNA delivery to Reduce alpha-Synuclein Expression in a Model of Parkinson's Disease. Mol. Ther. Nucleic Acids 9, 57–68.
Howard, D.B., et al., 2008. Tropism and toxicity of adeno-associated viral vector serotypes 1, 2, 5, 6, 7, 8, and 9 in rat neurons and glia in vitro. Virology 372, 24–34.
Klivenyi, P., et al., 2006. Mice lacking alpha-synuclein are resistant to mitochondrial toxins. Neurobiol. Dis. 21, 541–548.
Langston, J.W., et al., 1983. Chronic Parkinsonism in humans due to a product of meperidine-analog synthesis. Science 219, 979–980.
Makinen, P.I., et al., 2006. Stable RNA interference: comparison of U6 and H1 promoters in endothelial cells and in mouse brain. J. Gene Med. 8, 433–441.
McBride, J.L., et al., 2008. Artificial miRNAs mitigate shRNA-mediated toxicity in the brain: implications for the therapeutic development of RNAi. Proc. Natl. Acad. Sci. U. S. A. 105, 5868–5873.
McCormack, A.L., Mak, S.K., Henderson, J.M., Bumcrot, D., Farrer, M.J., et al., 2010. Alpha-synuclein suppression by targeted small interfering RNA in the primate substantia nigra. PLoS One 5 (8), e12122. https://doi.org/10.1371/journal.pone.0012122.
Mittal, S., et al., 2017. beta2-Adrenoreceptor is a regulator of the alpha-synuclein gene driving risk of Parkinson's disease. Science 357, 891–898.
Robertson, D.C., et al., 2004. Developmental loss and resistance to MPTP toxicity of dopaminergic neurones in substantia nigra pars compacta of gamma-synuclein, alpha-synuclein and double alpha/gamma-synuclein null mutant mice. J. Neurochem. 89, 1126–1136.
Satake, W., et al., 2009. Genome-wide association study identifies common variants at four loci as genetic risk factors for Parkinson's disease. Nat. Genet. 41, 1303–1307.
Schluter, O.M., et al., 2003. Role of alpha-synuclein in 1-methyl-4-phenyl-1,2,3,6-tetrahydropyridine-induced parkinsonism in mice. Neuroscience 118, 985–1002.
Scoles, D.R., et al., 2017. Antisense oligonucleotide therapy for spinocerebellar ataxia type 2. Nature 544, 362–366.
Simon-Sanchez, J., et al., 2009. Genome-wide association study reveals genetic risk underlying Parkinson's disease. Nat. Genet. 41, 1308–1312.
Singleton, A.B., et al., 2003. Alpha-Synuclein locus triplication causes Parkinson's disease. Science 302, 841.
Soldner, F., et al., 2016. Parkinson-associated risk variant in distal enhancer of alpha-synuclein modulates target gene expression. Nature 533, 95–99.
Specht, C.G., Schoepfer, R., 2001. Deletion of the alpha-synuclein locus in a subpopulation of C57BL/6J inbred mice. BMC Neurosci. 2, 11.
Spillantini, M.G., et al., 1997. Alpha-synuclein in Lewy bodies. Nature 388, 839–840.
Tanner, C.M., et al., 2011. Rotenone, paraquat, and Parkinson's disease. Environ. Health Perspect. 119, 866–872.
Tapias, V., Greenamyre, J.T., 2014. A rapid and sensitive automated image-based approach for in vitro and in vivo characterization of cell morphology and quantification of cell number and neurite architecture. Curr. Protoc. Cytom. 68 (12 33 1-12 33 22).
Tapias, V., et al., 2013. Automated imaging system for fast quantitation of neurons, cell morphology and neurite morphometry in vivo and in vitro. Neurobiol. Dis. 54, 158–168.
Ulusoy, A., et al., 2009. Dose optimization for long-term rAAV-mediated RNA interference in the nigrostriatal projection neurons. Mol. Ther. 17, 1574–1584.
Woodlee, M.T., et al., 2008. Enhanced function in the good forelimb of hemi-parkinson rats: compensatory adaptation for contralateral postural instability? Exp. Neurol. 211, 511–517.
Zharikov, A.D., et al., 2015. shRNA targeting alpha-synuclein prevents neurodegeneration in a Parkinson's disease model. J. Clin. Invest. 125, 2721–2735.